SYMPOSIUM

The Lateral Line System is Not Necessary for Rheotaxis in the Mexican Blind Cavefish (Astyanax fasciatus)

William J. Van Trump and Matthew J. McHenry[1]

Department of Ecology and Evolutionary Biology, 321 Steinhaus Hall, University of California at Irvine, Irvine, CA 92697-2525, USA

From the symposium "When Predators Attack: Sensing Motion in Predator-Prey Interactions" presented at the annual meeting of the Society for Integrative and Comparative Biology, January 3–7, 2013 at San Francisco, California.

[1]E-mail: mmchenry@uci.edu

Synopsis Fish resist being swept downstream by swimming against a current. Mexican blind cavefish (Astyanax fasciatus) exhibit this innate behavior, rheotaxis, without the aid of vision, but it has been debated whether this ability requires sensing flow with the lateral line system. We tested the role of the lateral line by comparing swimming in a flow chamber in a group of cavefish with a compromised lateral line with a control group. Consistent with previous studies, we found that cavefish orient toward flow and more frequently swim upstream at a higher flow speed. We found that these responses to flow were indistinguishable between fish with compromised and functioning lateral line systems. Rheotaxis was also unaltered by exposing fish to varying degrees of turbulence. These results suggest that the sensing of flow is unnecessary for rheotaxis in cavefish. It appears that tactile stimuli provide a sufficient means of executing this behavior in fish and that rheotaxis may not be a major function of the lateral line system.

Introduction

A fish resists being swept away by orienting its body counter to the direction of water flow and then swimming against the current. This innate behavior, rheotaxis, allows a fish to remain stationary with respect to the substrate in a dynamic aquatic environment. This response is exhibited by a broad diversity of freshwater and benthic and pelagic marine fishes (Arnold 1974) and appears at the earliest stages of life history (Olszewski et al. 2012). Therefore, rheotaxis is important for the biology of fishes and its sensory basis is of long-standing interest among biologists (Dijkgraaf 1963). The present study tests how rheotaxis is affected by the ability to sense water flow in the Mexican blind cavefish (Astyanax fasciatus, Characidae; Cuvier 1819), a species that relies on its lateral line system to orient to its environment.

Fish may execute rheotaxis via a variety of sensory systems. A component of this behavior, station-holding, is achieved when a fish minimizes its motion with respect to an earth-bound frame of reference. Vision can serve this function and allow a fish to swim against a current to avoid slipping with respect to a visual stimulus (Lyon 1904). Furthermore, fish will track a moving visual stimulus, irrespective of whether the water is stationary or moving (Russell 1934). However, fish also can execute rheotaxis by relying on mechanosensory cues. A fish in the dark will generally drift with a steady current until it comes in contact with a stationary surface, at which time the fish will orient and swim to minimize motion with respect to the surface (Lyon 1904).

Since the discovery of the lateral line system (Schulze 1861), biologists have debated whether it plays a role in rheotaxis. Dijkgraaf (1934) challenged earlier arguments that rheotaxis is an essential function of the lateral line (e.g., Hofer 1908) with his observation that its experimental ablation had no visible influence on the ability to perform rheotaxis under most circumstances. These experiments were later replicated in blind cavefish (Astyanax jordani, Hahn 1960), supporting the view that fish can achieve this behavior in the absence both of the lateral line and of visual stimuli.

This subject was revisited by Montgomery et al. (1997), with experiments that measured orientation

with respect to flow as a function of speed. They found that three distantly-related species of fish oriented to flows of relatively low speed. Furthermore, rheotaxis could be induced in fish with a compromised lateral line system, but it required a substantially higher rate of flow. This experimental design did not prevent fish from touching the substrate or viewing their surroundings. Therefore, these findings suggested that while tactile and visual cues may indicate motion relative to the substrate, the lateral line system is necessary for rheotaxis at low rates of flow.

This argument has been questioned by investigators who have scrutinized the experiments of Montgomery et al. (1997). Janssen (2000) found that the cobalt chloride treatment used by Montgomery et al. (1997), and Baker and Montgomery (1999), to block the lateral line was toxic, and sometimes fatal, to blind cavefish. This raised the possibility that behavioral changes induced by this preament had nothing to do with the lateral line. Janssen additionally argued that both studies relied on measuring the proportion of responses in a single group of fish for each species and thereby did not offer a statistically compelling case. The studies of Montgomery et al. (1997) and Baker and Montgomery (1999) also reported no effect of treating fish with gentamicin sulfate, which they considered to ablate only canal neuromasts and not the other type of lateral-line receptor, the superficial neuromasts. However, Van Trump et al. (2010) recently demonstrated that a treatment of gentamicin sulfate compromises the functioning of both types of receptors. This draws into question the view that rehotaxis is mediated by superficial neuromasts, and not by canal neuromasts as the earlier research suggested. The present study aimed to resolve the role of the lateral line system by revisiting the effect of gentamicin sulfate on rehotaxis in cavefish, using updated techniques.

If the sensing of flow is important to rheotaxis, then rheotaxis is likely to be affected by turbulence. Turbulence can provide a source of noise for the lateral line system if it offers random temporal fluctuations that hinder a fish's ability to resolve the direction and magnitude of prevailing currents (Engelmann et al. 2002; Kanter and Coombs 2003; Engelmann and Bleckmann 2004). Conversely, coherent vortices could offer a temporal signature that a fish could use to sense the velocity of flow as that pattern travels down the body (Chagnaud et al. 2006, 2007). In such circumstances, it is possible that turbulence could enhance rheotaxis by offering cues that would not exist in low turbulence. We have therefore tested whether rheotaxis differs between experimental treatments with different levels of turbulence.

Methods

Animals

Mexican blind cave fish, *Astyanax fasciatus* (3–7 cm, standard length) were obtained through a commercial fish supplier (Southland Aquatics, Inglewood, CA, USA) and housed in a custom-built recirculating aquarium system with clean, well-oxygenated fresh water at 19°C. Throughout experiments, animals were handled with care to avoid damaging the lateral line system. All experiments were performed in a flow chamber (Fig. 1A) filled with water drawn from the same reservoir that fed the aquaria and maintained at the same temperature.

Rheotaxis experiments

A recirculating flow chamber was used to generate flow of variable speed (Fig. 1A). Flow was generated by a propellor and passed through a cylindrical circuit with an opened section (150.0 cm long, 10.2 cm wide, and 11.4 cm deep) composed of clear acrylic, as described by Vogel (1981). In order to reduce the turbulence created by the chamber, we placed a working section (15.25 cm wide, 30.50 cm long, and 7.00 cm high) with pressure screens and flow collimators within the open section of the chamber. A course mesh barrier was inserted at the upstream and downstream edges of the visualization area to restrict animals within the working section and to prevent them from interacting with the turbulence-generating structures. In the absence of these structures, we were capable of generating low-turbulence currents in the center of the working section for flow speeds from 1 to $16 \, \mathrm{cm \, s}^{-1}$.

Rheotaxis was measured from video recordings of individual fish exposed to a range of increasing velocity of flow. Following a 30-min acclimation period, fish were exposed to each speed (0, 1, 2, 4, 6, 8, 10, 13, and $16 \, \mathrm{cm \, s}^{-1}$) for a duration of 5 min. The animals were video recorded from above at $7.5 \, \mathrm{frames \, s}^{-1}$ (Marlin F131B, AVT, Stadtroda, Germany). This sequence was performed on 12 fish with a disabled lateral-line system (see ''Antibiotic treatment'' below for details) and 10 control fish. Fish were made to swim in a series of increasing rates of flow instead of a randomized order so as to avoid sensitizing animals to the direction of flow early in the experimental trials. Supplemental experiments indicated no effect of learning on these measurements, as orientation did not vary with the number of repeated exposures to the same velocity of flow.
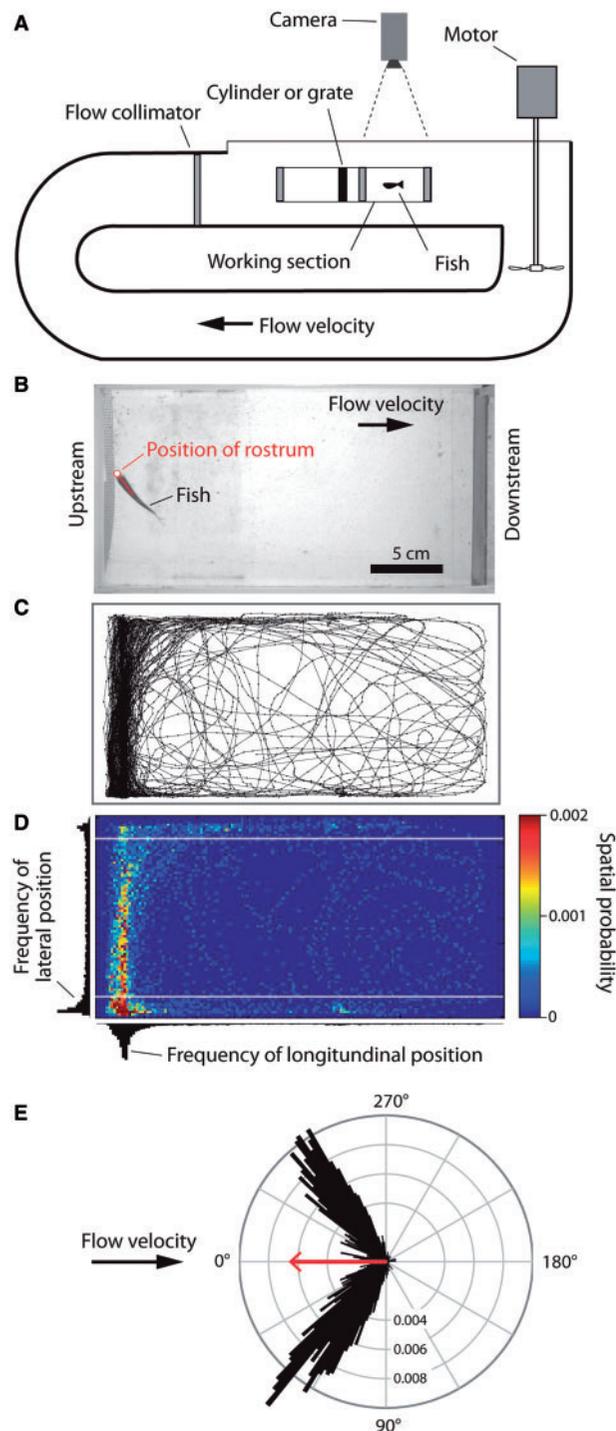
A separate group of fish was exposed to a sequence of different flow conditions to assess the role of turbulence on rheotaxis. Twenty-four animals were subjected to a 4-cm s^{-1} flow for 15 min under three different levels of turbulence (see "Turbulence treatments" below for details). The ordering of these treatments was randomized for each fish.

Rheotaxis was measured by analyzing the frequency of body position and of orientation within the working section of the flow chamber. A custom Matlab (ver. 2010a, Mathworks, Natick, MA, USA) program was used to automatically track the cranial position and orientation of a fish recorded in each video frame (Fig. 1B). This allowed for the collection of a large number of measurements for each animal (>1.5 million video frames total). To minimize the influence of interactions with the walls of the flow chamber, we excluded measurements of orientation for periods when fish were within 2 cm of a lateral wall. The trajectory of a fish (Fig. 1C) provided the basis for calculating the proportion of time the fish occupied a particular pixel of the video frame (Fig. 1D). The sum of these probability values along the transverse and longitudinal positions of the working sections provided frequency distributions along those dimensions. This method for representing spatial patterns in body position is identical to the transit probability histograms in previous studies on insects (Frye et al. 2003; Budick and Dickinson 2006). The upstream probability was calculated as the fraction of time during a trial an animal spent in the upstream quarter of the length of the working section. Orientation was analyzed to calculate a radial probability histograms, in the form of a rose plot (Fisher 1996). As with measurements of position, these histograms were constructed for each animal and then averaged to form a histogram of collective angular probability. To compare between treatments, each animal's measurements of body orientation from a trial were summed to calculate the resultant vector of all orientations during the test. This was done by considering each measured

Fig. 1 Experimental setup and kinematic analysis. (A) Schematic drawing of the flow tank with a working section that enclosed individual fish for video recording and that allowed for the control of turbulence. (B) A video frame from a representative recording of a fish exposed to a flow speed of 2 cm s^{-1}. The position of the rostrum (red circle) and body orientation (red line) were automatically tracked with custom software. (C) The trajectory of the fish's swimming was determined by tracking its position over 5 min, recorded at 7.5 frames s^{-1}. (D) The swimming trajectory in C is plotted as a psuedocolor map of spatial probability, equal to the proportion of time the fish occupied each pixel in the video recording. Therefore, the sum of all values

Fig. 1 Continued
mapped is equal to unity. The sum of longitudinal and lateral positions provides frequency distributions along each of those dimensions. Orientation values recorded within 2 cm of the lateral walls of the tank (gray lines) were discarded to minimize the influence of the walls on behavior. (E) A frequency distribution for body orientation indicates the proportion of time the fish was directed at particular angles. The mean vector (red arrow) has a magnitude that approaches unity as a fish spends a greater proportion of time in one direction. Colors refer to online version only.

body orientation as a unit vector with an angle corresponding to the major axis of the animal's body. Unit vectors were combined to yield a single resultant vector with an angle (θ) calculated with respect to the upstream direction.

Statistical tests determined differences in rheotaxis with speed and turbulence and by disabling the lateral line. Non-parametric tests were used for all comparisons of orientation and position, as the distributions of probabilities were found to differ from normal and von Mises distributions, respectively, even after arcsine transformation. In particular, spatial and radial probabilities were compared using Wilcoxon signed-rank tests (Sokal and Rohlf 1995). All statistical analyses were conducted with a custom Matlab program.

Antibiotic treatment

We pharmacologically ablated the lateral line system with an antibiotic to study its role in rheotaxis. A group of animals was exposed to a solution of 0.002% gentamicin sulfate (Fisher Scientific, Pittsburgh, PA) for 18 h in a 5-l tank containing fresh, well-oxygenated water. This treatment has been shown to block the functioning of the lateral line system in A. fasciatus (Van Trump et al. 2010) and we confirmed its effectiveness both with behavioral assays and fluorescence microscopy. Unlike control fish, treated fish failed to respond to a fluid jet and they collided with walls and occasionally swam perpendicular to a wall with their rostrum against the tank. We visualized the hair cells of the lateral line in three randomly-selected fish from treated and control groups by anesthetizing the animals (with $200 \, \mathrm{mg \, l^{-1}}$ MS-222, Argent Labs, Redmond, WA, USA) and exposing them to a 0.008% DASPEI (2-[4-(dimethylamino)styryl]-N-ethylpyridinium iodide; Molecular Probes, Eugene, OR, USA) solution (Harris et al. 2003; Murakami et al. 2003). Hair cells were visualized with a fluorescence stereomicroscope (Zeiss Discovery V.20, Carl Zeiss, Thornwood, NY, USA) using a GFP filter set (excitation 450–490 nm and barrier 515 nm). Consistent with prior findings (Van Trump et al. 2010), the gentamicin treatment substantially disrupted the functioning hair cells in both superficial and canal neuromasts throughout the body. All behavioral trials were completed within 3 h of the treatment so that hair cells were not permitted to substantially regenerate (Harris et al. 2003; McHenry et al. 2009).

Turbulence treatments

We exposed fish to three flow treatments to test the effect of turbulence on rheotaxis. The "low turbulence"

treatment was no different from the control experiments described above, in which we used a flow speed of $4 \, \mathrm{cm \, s^{-1}}$. Our "high turbulence" treatment was generated by a PVC pipe (3 cm in diameter) placed vertically in center of the chamber, 4 cm upstream of the working section. Instead of this cylinder, a grate (in sections $3 \, \mathrm{cm^2}$) was placed upstream at $45°$ with respect to the flow to create "asymmetric turbulence". Our measurements of flow visualization showed that the spatial mean of flow speed was consistent across these turbulence conditions.

Digital particle image velocimetry (DPIV) was used to measure flow speed and turbulence. Water within the flow chamber was seeded with neutrally-buoyant hollow silvered glass spheres ($44 \, \mu m$, Potters Industries, Carlstadt, NJ, USA). These were illuminated by a $\sim$2-mm-thick sheet of laser light (2 W DPSS Nd:YAG laser; Quantum Excel; Laser Quantum Ltd, Stockport, Cheshire, UK) and filmed from above at 200 frames $\mathrm{s^{-1}}$ with high spatial resolution (1024×512 pixels, Photron Fastcam 1024, Photron USA, San Diego, CA, USA) for 15 s. Flow velocity fields were calculated from these video recordings with DPIV software (OSIV; osiv.sourceforge.net). Every eighth frame was analyzed and compared to a frame 2, 4, or 8 ahead in the sequence, depending on the particles' speed. We used a direct-normalized correlation algorithm for the cross-correlation of 32×32 pixel interrogation windows between frames. The intensity of turbulence (I) was calculated for each interrogation window for a period ($T = 15 \, \mathrm{s}$) of measurements of the velocity of flow. Turbulence intensity was calculated as the standard deviation of flow velocity (u) in direction of freestream flow, divided by the time-averaged downstream velocity ($\bar{u}$, Munson et al. 2002):

$$I = \frac{1}{\bar{u}} \sqrt{\frac{1}{T} \int_0^T (u - \bar{u})^2 \, dt}. \qquad (1)$$

Results

Response to the velocity of flow

The cave fish explored the working section of the flow tank in the absence of flow. A fish placed in the working section initially swam rapidly around the enclosure. By the end of the 30-min acclimation period, the swimming speed had visibly decreased, but the fish remained active by moving around the working section with a preference for swimming along the lateral walls, collimators, and corners of the tank (Fig. 1B–E). In the absence of flow ($0 \, \mathrm{cm \, s^{-1}}$ in Fig. 2A), fish occupied the upstream and downstream
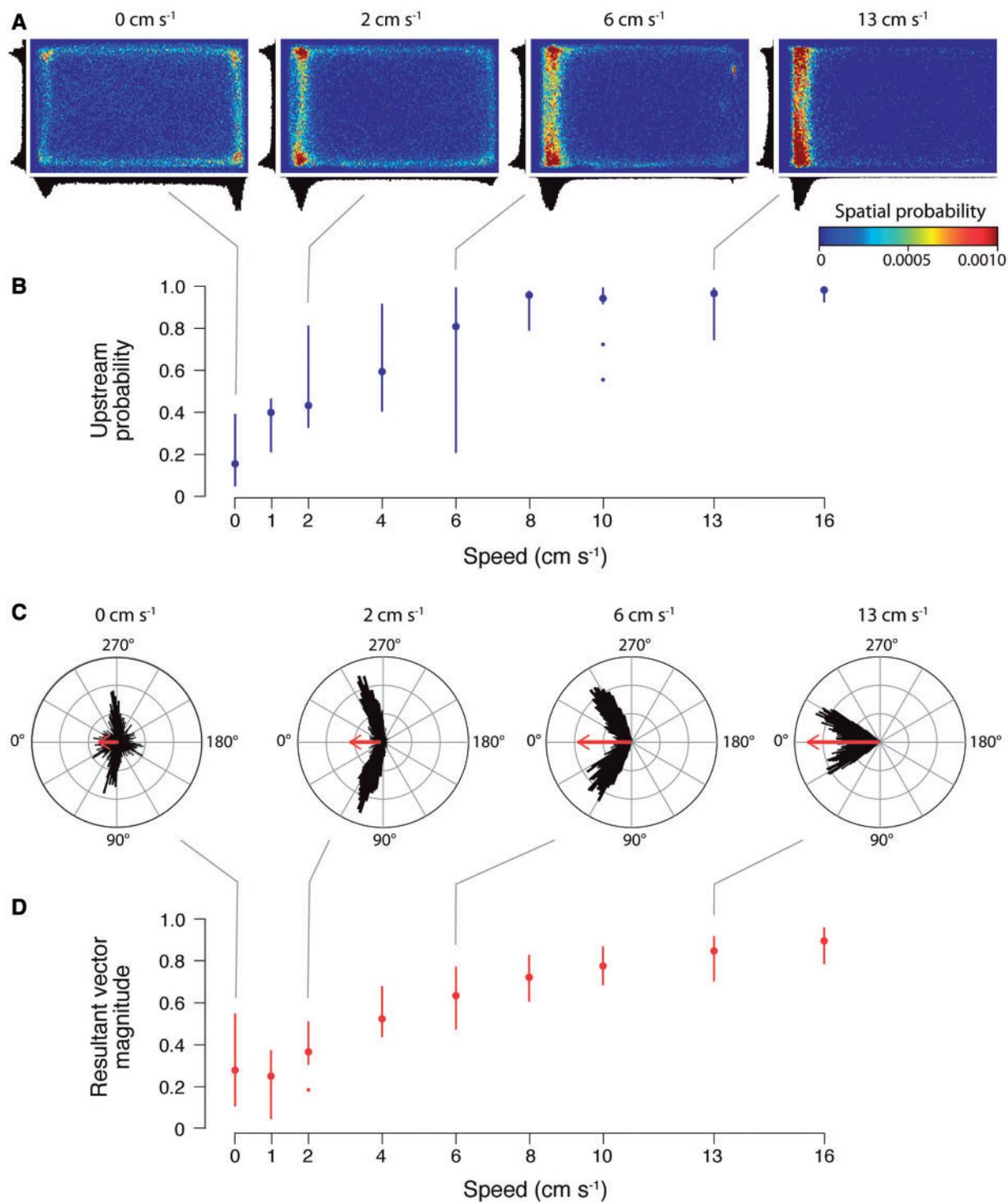
Fig. 2 Rheotaxis in Mexican blind cavefish is reflected in the spatial probability (A, B) and frequency distribution of orientation (C, D) in a group of fish ($N = 10$) made to swim when exposed to different speeds of flow. (A) Position probability at four flow speeds (0, 2, 6, and 13 cm s^{-1}) illustrate where in the working section (Fig. 1A) fish spent the greatest proportion of their time. (B) The upstream probability, equal to the proportion of time spent in the upstream region (the first 25% of the length), increased monotonically with flow speed. (C) Histograms of orientation probability indicate the frequency distribution of body direction. The resultant vector (red arrow) indicates the average body orientation with a length scaled to the radius of the rose plot. (D) The magnitude of this vector increased with speed as the fish's swimming became more directed upstream. (B and D) Measurements are represented by the median (filled circle), range (vertical line), and outliers (dots, values greater than 1.5 quartiles from the median).

ends of the working section with a slight bias toward the downstream end (Fig. 2A). Measurements of the orientation of the body exhibited two large modes in the lateral directions (around $\theta = 90°$ and $\theta = 270°$ for $0\,\text{cm s}^{-1}$ in Fig. 2C), from swimming normal to the lateral walls and along the collimators. Two smaller modes appeared around the longitudinal directions ($\theta = 0°$ and $\theta = 180°$), which reflects the proportion of time spent following along the lateral walls and normal to the collimators.

When exposed to water flow, fish spent more time in the upstream portion of the chamber and began to swim with a tacking pattern. This consisted of lateral motion toward one wall, touching that wall, and then traversing to the opposite wall. This tacking occurred with increasing frequency at the upstream end of the working section as velocity of flow increased, as shown by a monotonic increase in upstream probability with increasing flow speed ($P < 0.05$ for all individuals; Kendall's nonparametric regression, Fig. 2B). Values for upstream probability were significantly greater than in the absence of flow for all but the lowest speed of flow ($1\,\text{cm s}^{-1}$, $P = 0.30$; $2–16\,\text{cm s}^{-1}$, $P \ll 0.01$; $N = 12$).

The tacking pattern of cavefish creates a bimodal distribution of body orientations (Fig. 2C). One mode corresponds to instances when an animal is tacking right ($180° < \theta < 360°$) and the other when tacking left ($0° < \theta < 180°$). As flow speed increased, these two modes shifted upstream (i.e., toward $\theta = 0°$), with the two modes fusing to form a diffuse unimodal distribution at the highest speeds (e.g., $13\,\text{cm s}^{-1}$ in Fig. 2C and D). Due to the mirror symmetry of the bimodal distribution, the angle of the resultant vector was nearly zero for all speeds (red arrow in Fig. 2C). However, the magnitude of this vector increased with speed as the distribution of body orientation clustered closer to the upstream direction (Fig. 2D). This magnitude of the vector was significantly different from the value measured in the absence of flow, for speeds greater than $2\,\text{cm s}^{-1}$ ($1\,\text{cm s}^{-1}$, $P = 0.47$; $2\,\text{cm s}^{-1}$, $P = 0.05$; $4–16\,\text{cm s}^{-1}$, $P \ll 0.01$; $N = 12$; Kendall's nonparametric regression, $P < 0.05$).

Effects of gentamicin sulfate

We treated fish with gentamicin sulfate to compromise the functioning of the lateral line and thereby test its role in rheotaxis. Treated fish appeared to swim more erratically, with frequent spontaneous turns and occasional spiraling. Wall-following was less frequent and treated fish collided with walls more often (Fig. 3A) than did control fish

(Fig. 2A). Despite these differences, kinematics varied with flow speed in a manner similar to the results from control fish. As in control fish, treated fish demonstrated a greater upstream probability than in the absence of flow, for all but the lowest speed ($1\,\text{cm s}^{-1}$: $P = 0.05$; $2–16\,\text{cm s}^{-1}$: $P \ll 0.01$; $N = 12$; Fig. 4 A and B). Furthermore, the upstream probability was indistinguishable from that of the control group at all flow speeds ($P > 0.05$, $N = 12$, Wilcoxon signed-ranks test), but one ($13\,\text{cm s}^{-1}$, $P = 0.03$, $N = 12$). As in control fish, treated fish showed an elevated vector magnitude for flows greater than $1\,\text{cm s}^{-1}$ ($1\,\text{cm s}^{-1}$: $P = 0.07$, $2–16\,\text{cm s}^{-1}$: $P \ll 0.01$, $N = 12$, Fig. 4D) and the values of this magnitude were indistinguishable between the two groups ($1–16\,\text{cm s}^{-1}$: $P > 0.05$, $N = 12$), except in the absence of flow ($0\,\text{cm s}^{-1}$: $P = 0.04$, $N = 12$).

Response to turbulence

The different flow treatments generated distinct spatial patterns of turbulence (Fig. 4A). In our low turbulence treatment, relatively high turbulence was only observed near the lateral walls. Almost the opposite pattern was created by the high turbulence treatment, during which the cylinder created turbulence that was greatest through the center of the chamber but slight near the walls (Fig. 4A). This turbulence took the form of a von Kármán vortex street. A third pattern of flow was created by asymmetric turbulence, during which an angled grate created high turbulence near the right wall of the working section, with low turbulence on the left wall.

Despite these differences in the spatial pattern of turbulence, cavefish demonstrated similar orientation for all treatments (Fig. 3). The left and right tacking modes were considered separately (symmetry analysis based on Wilcoxon sign-rank statistic; Fisher 1996) and the magnitude of the upstream component of the resultant vector was calculated for each mode as a measure of the strength of orientation. For both low and high turbulence, there was no detectable difference in orientation-strength of the two modes (Fig. 4D; $P > 0.05$, $N = 24$). Additionally, there was no detectable difference in orientation-strength (Fig. 4D; $P > 0.05$, $N = 24$) or upstream bias (Fig. 4E; $P > 0.05$, $N = 24$) between high, asymmetric, and low turbulence.

Cavefish did not prefer, or avoid, areas of increased turbulence within the working section of the flow chamber. Despite greater turbulence in the center of the flow chamber under high turbulence, the fraction of time animals spent in the center half
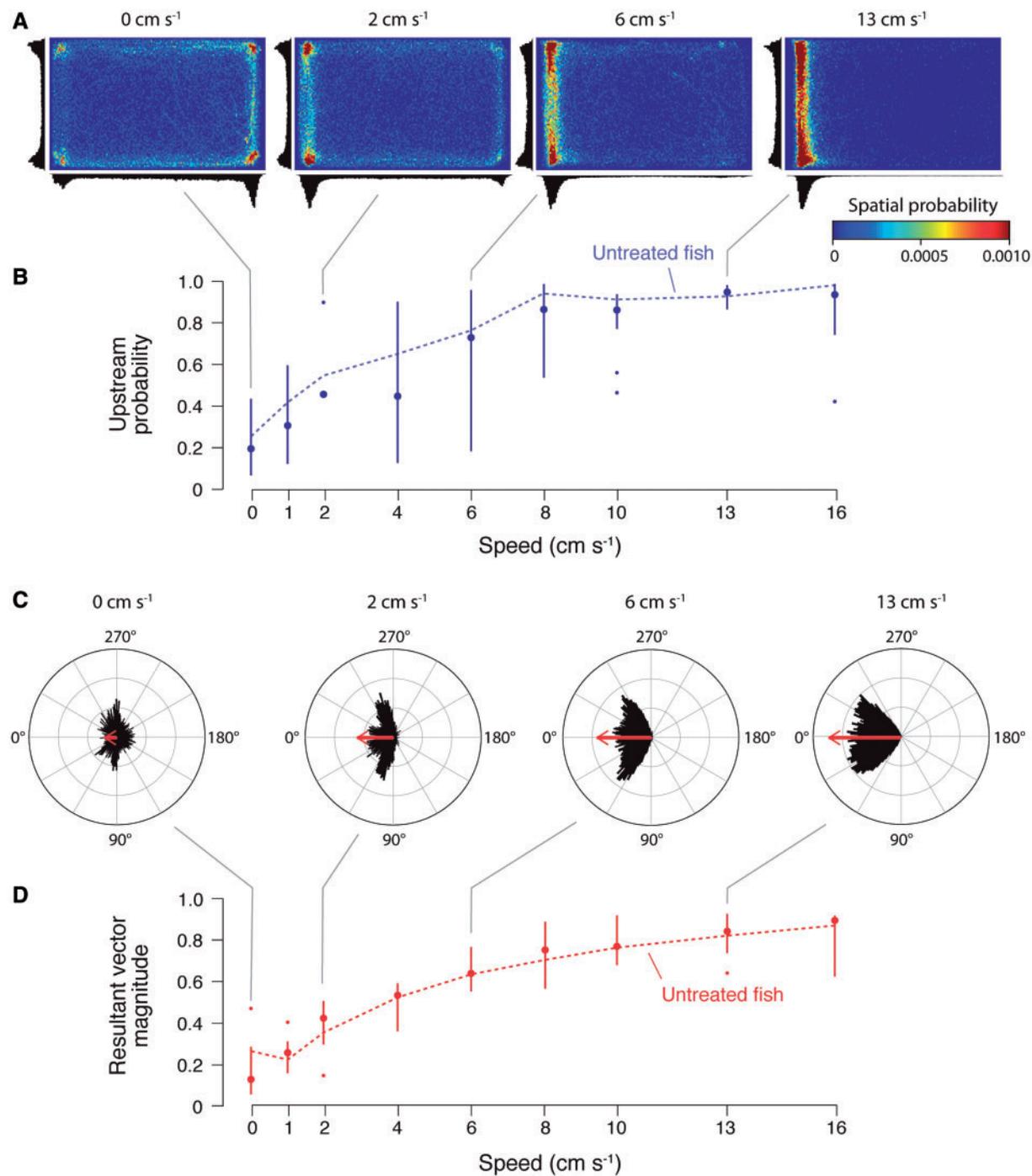
Fig. 3 Rheotaxis in cavefish with a compromised lateral line system. Measurements of the position (**A**, **B**) and direction (**C**, **D**) of swimming are shown for a group ($N = 12$) of fish treated with gentamicin sulfate to block the functioning of the hair cells in their lateral line system. (**A**) Position probability at four flow speeds (0, 2, 6, and 13 cm s^{-1}) illustrate where in the working section (Fig. 1A) fish spent the greatest proportion of time. (**B**) The upstream probability, equal to the proportion of time spent in the upstream region (the first 25% of the length), increased monotonically with flow speed. These measurements are similar to the mean values of upstream probability for untreated fish (dashed line). (**C**) Histograms of orientation probability indicate the frequency distribution of body direction. The resultant vector (red arrow) indicates the average orientation of the body with a length scaled to the radius of the rose plot. (**D**) The magnitude of this vector increased with speed as the fish's swimming became more directed upstream. These measurements are similar to the mean magnitude of the vector for untreated fish (dashed line). (**B** and **D**) Measurements are represented by the median (filled circle), range (vertical line), and outliers (dots, values greater than 1.5 quartiles from the median).

of the chamber was indistinguishable from that of low turbulence ($P < 0.05$, $N = 24$). Similarly, fish did not exhibit a preference for the right side (i.e., high turbulence) or the left side (i.e., low turbulence) of the chamber under asymmetric turbulence (Fig. 4B; $P = 0.22$, $N = 24$). Likewise, both under low and high turbulence, fish did not prefer the either the left or the right side of the tank (Fig. 4B; $P > 0.05$, $N = 24$). Despite this lack of a preference for position in the chamber, fish under asymmetric turbulence did show a stronger orienting response when tacking right than when tacking left, (Fig. 4C; $P \ll 0.01$, $N = 24$).

Discussion

The lateral line system is not necessary for rheotaxis

Our measurements of rheotaxis are consistent with prior studies on blind cavefish. We found that cavefish directed their swimming toward flow (Fig. 2D) and were positioned in the upstream direction with greater frequency (Fig. 2B) as flow speed increased. Similar patterns were reported by Montgomery et al. (1997) and Baker and Montgomery (1999). They found that the proportion of fish aligned with flow increased with speed and that this pattern was unchanged by a treatment of gentamicin sulfate.

Despite this similarity in results, we presently offer different conclusions due to a revised interpretation of the effects of gentamicin sulfate. Earlier studies used scanning electron microscopy and light microscopy to assess the influence of pharmacological treatments on the functioning of the lateral line (Song et al. 1995). Based on those techniques, previous studies on cavefish and other species interpreted a gentamicin treatment as affecting only the hair cells within canal neuromasts, but not those in superficial neuromasts (e.g., Coombs et al. 2001; Montgomery et al. 2002). Therefore, the lack of an effect of gentamicin on rheotaxis in cavefish was interpreted as an indication that this behavior did not depend on canal neuromasts (Montgomery et al. 1997; Baker and Montgomery 1999). Furthermore, these studies reported that a physical ablation of superficial neuromasts and a treatment of cobalt chloride (which disables both types of neuromast; Karlsen and Sand 1987) caused cavefish to have a higher threshold speed for rheotaxis. It was therefore concluded that rheotaxis depends on the functioning of superficial neuromasts, but not on canal neuromasts.

Our conclusion is that neither superficial neuromasts nor canal neuromasts are necessary for rheotaxis in blind cavefish. This conclusion is based on our finding that gentamicin sulfate disables both types of neuromast. This treatment was developed, and presently confirmed, through the use of DASPEI staining (Van Trump et al. 2010). This fluorescent vital stain offers a comprehensive measure of the functioning of hair cells in vivo (Harris et al. 2003; Murakami et al. 2003). It indicates that our gentamicin treatment massively reduces the number of functional hair cells both within canal neuromasts and superficial neuromasts (Van Trump et al. 2010). This was found even for exposures of shorter duration and of lower concentrations than previously employed (Montgomery et al. 1997; Baker and Montgomery 1999).

The present study does not offer direct insight into why other manipulations of the lateral line system have been reported to affect rheotaxis in cavefish. Janssen (2000) argued against drawing conclusions from the cobalt chloride treatment used by Montgomery et al. (1997) and Baker and Montgomery (1999) because it was found to be toxic to blind cavefish. Janssen further questioned the validity of all findings in those studies due to pseudoreplication in the statistical design. It is additionally possible that the reported rise in threshold speed caused by a physical ablation (Baker and Montgomery 1999) could have been caused by the additional handling required for this treatment, as no sham surgeries were reported. This issue would best be resolved by an attempt to replicate the ablation experiments of Baker and Montgomery (1999) with the updated kinematic measurements used presently, and by comparing treated fish with those exposed to sham surgeries and an unmanipulated control. Nonetheless, our results offer a compelling case that neither type of neuromast is necessary for rheotaxis in blind cavefish.

Rheotaxis may be important for the survival of Mexican blind cavefish during seasonal periods of high flow. Numerous cave systems are inhabited by *Astyanax fasciatus* in the karst landscape in northeastern Mexico, where water flows into adjacent streams (Mitchell et al. 1977). Although water within the caves is stagnant or flows very slowly for much of the year, this changes during seasonal periods of high rainfall when caves routinely flood (Breder 1942; Mitchell et al. 1977). This presents a danger to the cavefish because their lack of vision and pigmentation would presumably expose them to predation and would put them at a competitive disadvantage against stream-dwelling species. Rheotaxis would therefore appear to be an essential behavior for this species.
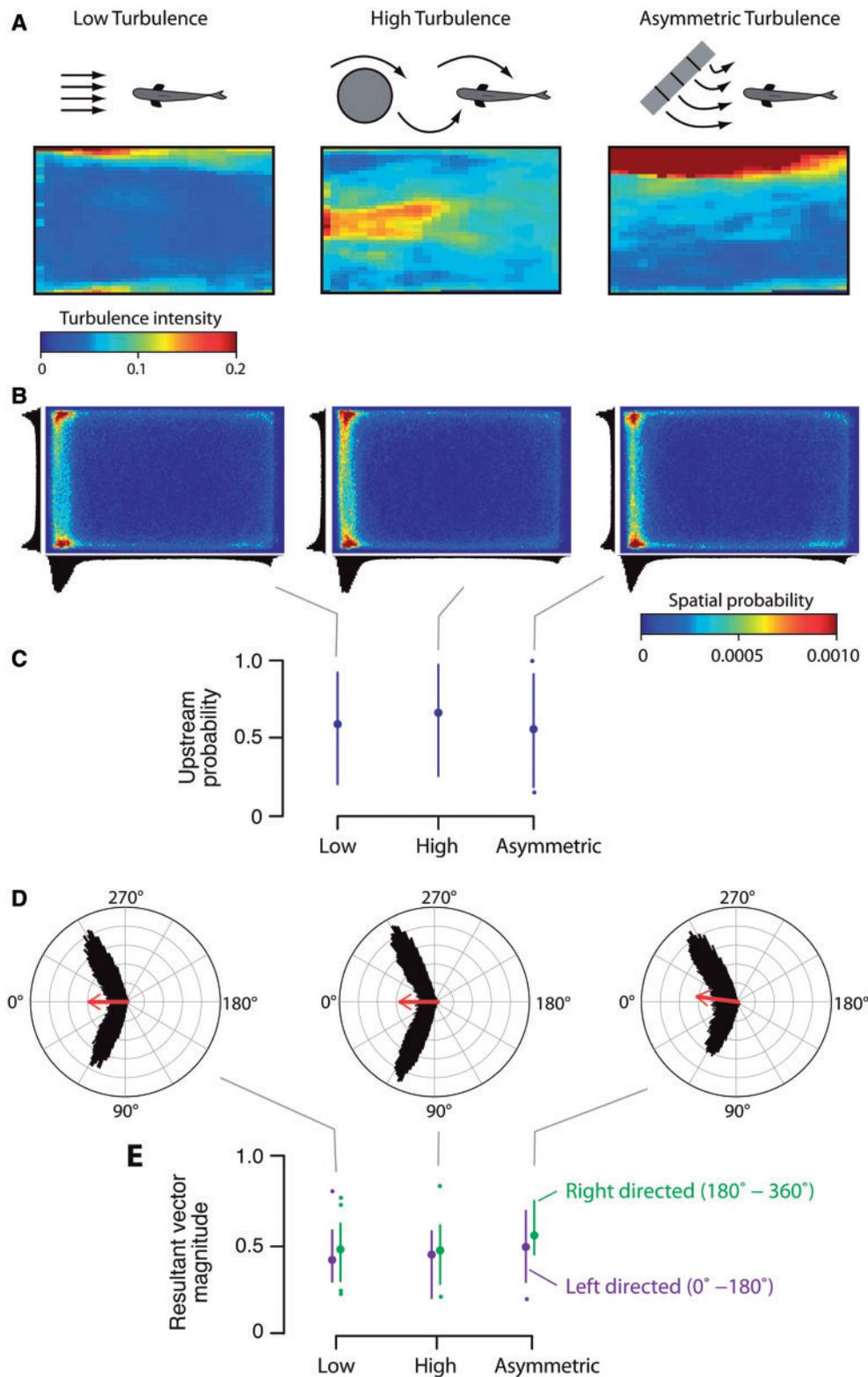
Fig. 4 The effects of turbulence on rheotaxis. (**A**) The intensity of turbulence, measured with DPIV, is shown for three flows. All treatments used a mean flow speed of $4\,\mathrm{cm\,s^{-1}}$, which approximates the threshold for rheotaxis in blind cavefish (Baker and Montgomery 1999). (**B**) The spatial probability demonstrates the proportion of time spent in each region of the working section ($N = 24$). (**C**) The upstream probability, equal to the proportion of time spent in the upstream region (the first 25% of the length) is shown for each treatment. (**D**) Histograms of orientation probability indicate the frequency distribution of body direction. The resultant vector (red arrow) indicates the average body orientation with a length scaled to the radius of the rose plot. (**E**) The upstream component of the left-directed ($0°–180°$, in purple) and right-directed ($180°–360°$, in green) orientation values are compared. (**C** and **E**) Measurements are represented by the median (filled circle), range (vertical line), and outliers (dots, values greater than 1.5 quartiles from the median). Colors refer to online version only.

Rheotaxis may not be affected by turbulence

We found no evidence to suggest that rheotaxis is affected by turbulent conditions. Our measurements revealed similar results in terms of the position (Fig. 4B and C) and the direction (Fig. 4D and E) of swimming for our three flow treatments. Therefore, cavefish did not show either a preference for or aversion to high turbulence. This result is perhaps not surprising in light of our finding that rheotaxis is not mediated by the lateral line system. If flow sensing does not influence this behavior, then turbulence cannot serve either as a source of noise or as a means of enhancing the flow signal (Engelmann et al. 2002; Kanter and Coombs 2003; Engelmann and Bleckmann. 2004; Chagnaud et al. 2006, 2007).

Our experiments do leave open the possibility for turbulence to affect rheotaxis by jostling the fish. Such a direct mechanical perturbation might be expected in highly energetic flows, which could challenge the propulsive abilities of a fish to direct swimming and maintain equilibrium. This effect of turbulence would therefore influence rheotaxis directly and not by acting on sensory function. For our turbulence experiments, in order to maximize the possibility for detecting a measurable influence on lateral-line function, we chose to focus on a flow speed ($4\,\mathrm{cm\,s^{-1}}$) that is just above the threshold previously reported (Baker and Montgomery 1999). Higher flow speeds would have to be considered if one is interested in testing the effects of turbulence on propulsion.

The sensory basis of rheotaxis

If the lateral line system proves to be unnecessary for rheotaxis in other species, then we can turn to classic studies to understand how fish achieve this behavior. When exposed to flow, a fish that can see will attempt to hold station by swimming with a speed and direction that minimizes the visual appearance of motion induced by the current (Lyon 1904). This optokinetic behavior is obviously challenged in a darkened environment, but a fish can compensate by using mechanosensory cues. Fish attempt to hold station when coming into contact with a stationary surface in the dark, which suggests a role for the sense of touch (Arnold 1974). In addition, the vestibular system could assist in instances when the body is accelerated by fluid forces.

Although these modalities would appear to be sufficient for rheotaxis, they do not preclude a possible role for the lateral line system. Dijkgraaf (1934) observed that minnows use the lateral line to swim toward a relatively slow jet of fluid. Similarly, Olszewski et al. (2012) found the lateral line to be necessary for rheotaxis in zebrafish larvae when swimming away from a drain. In both of these instances, the flow field likely exhibited substantial variation across the length of the fish's body. Therefore, by integrating spatial cues, the lateral line system could aid in rheotaxis under special conditions. Nonetheless, such observations are consistent with Dijkgraaf's (1963) asssertion that "...although the lateral lines can indeed participate in the orientation of fishes towards currents as real rheotactic receptors, they are certainly less important in this connexion than the eye and the skin...".

Acknowledgments

Funding

References

Arnold GP. 1974. Rheotropism in fishes. Biol Rev Camb Philos Soc 49:515–76.

Baker CF, Montgomery J. 1999. The sensory basis of rheotaxis in the blind Mexican cave fish, *Astyanax fasciatus*. J Comp Physiol 184:519–27.

Breder C. 1942. Descriptive ecology of La Cueva Chica, with especial reference to the blind fish. Anoptichthys Zoologica 27:7–15.

Budick SA, Dickinson MH. 2006. Free-flight responses of *Drosophila melanogaster* to attractive odors. J Exp Biol 209:3001–3017.

Chagnaud BP, Bleckmann H, Engelmann J. 2006. Neural responses of goldfish lateral line afferents to vortex motions. J Exp Biol 209:327–42.

Chagnaud BP, Bleckmann H, Hoffman MH. 2007. Kármán vortex street detection by the lateral line. J Comp Physiol A 193:753–63.

Coombs S, Braun CB, Donovan B. 2001. The orienting response of Lake Michigan mottled sculpin is mediated by canal neuromasts. J Exp Biol 204:337–48.

Dijkgraaf S. 1934. Untersuchungen über die Funktion der Seitenorgane an Fischen. A Vergl Physiol 20:162–214.

Dijkgraaf S. 1963. Functioning and significance of lateral-line organs. Biol Rev 38:51–105.

Engelmann J, Bleckmann H. 2004. Coding of lateral line stimuli in the goldfish midbrain in still and running water. Zoology (Jena) 107:135–51.

Engelmann J, Hanke W, Bleckmann H. 2002. Lateral line reception in still- and running water. J Comp Physiol A 188:513–26.

Fisher NI. 1996. Statistical analysis of circular data. London: Cambridge University Press.

Frye MA, Tarsitano M, Dickinson MH. 2003. Odor localization requires visual feedback during free flight in Drosophila melanogaster. J Exp Biol 206:843–855.

Hahn G. 1960. Ferntastsinn und Strömungssinn beim augenlosen Höhlenfisch Anoptichthys jordani Hubbs und Innes im Vergleich zu einigen Teleosteern. Naturwissenschaften 47:611.

Harris JA, Cheng AG, Cunningham LL, MacDonald G, Raible DW, Rubel EW. 2003. Neomycin-induced hair cell death and rapid regeneration in the lateral line of zebrafish (Danio rerio). J Assoc Res Otolaryngol 4:219–34.

Hofer B. 1908. Studien über die Hautsinnesorgane der Fische. I. Die Funktion der Seitenorgane bei den Fischen. Ber Kgl Bayer Biol Versuchsstation Munchen 1:115–64.

Janssen J. 2000. Toxicity of Co2+: implications for lateral line studies. J Comp Physiol A 186:957–60.

Kanter MJ, Coombs S. 2003. Rheotaxis and prey detection in uniform currents by Lake Michigan mottled sculpin (Cottus bairdi). J Exp Biol 206:59–70.

Karlsen HE, Sand O. 1987. Selective and reversible blocking of the lateral line in freshwater fish. J Exp Biol 133:249–62.

Lyon EP. 1904. On rheotropism I. Rheotropism in fishes. Am J Physiol 12:149–61.

McHenry MJ, Feitl KE, Strother JA, Van Trump WJ. 2009. Larval zebrafish rapidly sense the water flow of a predator's strike. Biol Lett 5:477–9.

Mitchell RW, Russell WH, Elliott WR. 1977. Mexican eyeless characin fishes, genus Astyanax: environment, distribution, and evolution. Lubbock (TX): Texas Tech Press.

Montgomery J, Baker CF, Carton AG. 1997. The lateral line can mediate rheotaxis in fish. Nature 389:960–3.

Montgomery J, Macdonald F, Baker CF, Carton AG. 2002. Hydrodynamic contributions to multimodal guidance of prey capture behavior in fish. Brain Behav Evol 59:190–8.

Munson BR, Young DF, Okiishi TH. 2002. Fundamentals of fluid mechanics. New York: John Wiley & Sons, Inc.

Murakami SL, Cunningham LL, Werner LA, Bauer E, Pujol R, Raible DW, Rubel EW. 2003. Developmental differences in susceptibility to neomycin-induced hair cell death in the lateral line neuromasts of zebrafish (Danio rerio). Hear Res 186:47–56.

Olszewski J, Haehnel M, Taguchi M, Liao JC. 2012. Zebrafish larvae exhibit rheotaxis and can escape a continuous suction source using their lateral line. PLoS One 7:e36661.

Owens KN, Cunningham DE, Macdonald G, Rubel EW, Raible DW, Pujol R. 2007. Ultrastructural analysis of aminoglycoside-induced hair cell death in the zebrafish lateral line reveals an early mitochondrial response. J Comp Neurol 502:522–43.

Russell S. 1934. The behaviour of animals. London: Arnold. p. 184.

Schulze F. 1861. Über die Nervenendigung in den sogenannten Schleim-Kanälen der Fische und über entsprechende Organe der durch Kiemen atmenden Amphibien. Arch Anat u Phys:759–69.

Sokal RR, Rohlf FJ. 1995. Biometry: the principles and practice of statistics in biological research. New York (NY): W.H. Freeman.

Song J, Yan HY, Popper AN. 1995. Damage and recovery of hair cells in fish canal (but not superficial) neuromasts after gentamicin exposure. Hear Res 91:63–71.

Van Trump WJ, Coombs S, Duncan K, McHenry MJ. 2010. Gentamicin is ototoxic to all hair cells in the fish lateral line system. Hear Res 261:42–50.

Vogel S. 1981. Life in moving fluids. Princeton (NJ): Princton Univeristy Press.